Research Article Vol. 6, No. 4 / April 2019 / Optica 430

optica

Ultra-low threshold InAs/GaAs quantum dot microdisk lasers on planar on-axis Si (001) substrates

TAOJIE ZHOU,[1,†] MINGCHU TANG,[2,†] GUOHONG XIANG,[1] XUAN FANG,[1] XIU LIU,[1] BOYUAN XIANG,[1] SUIKONG HARK,[1] MICKAEL MARTIN,[3] MARIE-LEONOR TOURATON,[3,4] THIERRY BARON,[3] YING LU,[2] SIMING CHEN,[2,5] HUIYUN LIU,[2,6] AND ZHAOYU ZHANG[1,*]

[1]School of Science and Engineering, The Chinese University of Hong Kong, Shenzhen, Guangdong, 518172, China
[2]Department of Electronic and Electrical Engineering, University College London, London, WC1E 7JE, UK
[3]Université Grenoble Alpes, CNRS, CEA-LETI, MINATEC, LTM, F-38054 Grenoble, France
[4]STMicroelectronics, 850 rue Jean Monnet, F-38926 Crolles Cedex, France
[5]e-mail: siming.chen@ucl.ac.uk
[6]e-mail: huiyun.liu@ucl.ac.uk
*Corresponding author: zhangzy@cuhk.edu.cn

Received 22 October 2018; revised 5 March 2019; accepted 11 March 2019 (Doc. ID 348694); published 3 April 2019

Monolithic integration of efficient III–V light-emitting sources on planar on-axis Si (001) has been recognized as an enabling technology for realizing Si-based photonic integrated circuits (PICs). The field of microdisk lasers employing quantum dot (QD) materials is gaining significant momentum because it allows massive-scalable, streamlined fabrication of Si-based PICs to be made cost effectively. Here, we present InAs/GaAs QD microdisk lasers monolithically grown on on-axis Si (001) substrate with an ultra-low lasing threshold at room temperature under continuous-wave optical pumping. The lasing characteristics of microdisk lasers with small diameter (*D*) around 2 μm and sub-wavelength scale (*D*∼1.1 μm) are demonstrated, with a lasing threshold as low as ∼3 μW. The promising lasing characteristics of the microdisk lasers with ultra-low power consumption and small footprint represent a major advance towards large-scale, low-cost integration of laser sources on the Si platform.

https://doi.org/10.1364/OPTICA.6.000430

1. INTRODUCTION

The advanced technology of silicon photonics has emerged as a promising candidate for next-generation chip-scale data-communication networks and data centers [1–4]. Due to the in-direct band gap property of bulk group-IV materials, the integration of well-established III–V photonic devices on silicon is a promising solution to realize efficient Si-based light-emitting sources. Although the method of heterogeneous integration has been widely studied and developed [5,6], the method of monolithic integration is still preferred for low-cost and dense photonic integrated circuits (PICs) [7], which is challenged by the conjunction of large thermal, lattice, and polarity mismatches between the Si substrate and III–V layer [8,9]. Studies on the optimization of the III–V buffer layer have been performed [10,11], which have led to the demonstration of high-performance InAs/GaAs quantum dot (QD) lasers epitaxially grown on different types of intermediate buffer layers (GaAs, GaP, and Ge) and Si substrates, including off-cut (4°–6°) Si [12–16], patterned on-axis Si (001) [17–24], Ge-on-Si [25–30], and GaP/Si (001) substrates [31,32]. Very recently, we demonstrated InAs/GaAs QD ridge-waveguide lasers monolithically grown on CMOS-compatible, on-axis Si (001) substrate with only III-As buffer layers [33], which represents a major advance towards the commercial success of Si-based photonic-electronic integration. In order to interconnect the active region of laser devices and Si-based passive components, the thick buffer layer needs to be overcome. The interconnection between these parallel planes can be achieved by using a photonic wire bonding method [34] or introducing a grating coupler for vertical light coupling in the Si plane [35]. In addition, other possible solutions have been demonstrated, such as using a hybrid integration method by combining the bonding method and monolithic growth [36] and applying epitaxial lateral overgrowth technology [37].

Compared with ridge-waveguide lasers or distributed feedback lasers monolithically grown on Si, whispering-gallery-mode (WGM) microdisk lasers with small footprint configurations and ultra-low threshold allow for incorporating compact and efficient laser sources on a CMOS-compatible platform. Recently, *Wan et al.* reported continuous-wave (CW) optically pumped QD microdisk lasers under 10 K with a threshold of 35 μW [19] and CW lasing emission under room temperature with a lasing threshold of 200 μW [21,38], in which the five stacked

InAs QD active layers were directly grown on a GaAs-on-V-grooved-Si template with emission around 1.3 μm. *Li et al.* presented CW optically pumped microdisk lasers with five layers of QDs as gain material grown on exact Si (001) substrate, and a lasing threshold of ∼652 μW was obtained at room temperature [20]. *Shi et al.* demonstrated a 1.55 μm QD microdisk laser grown on an on-axis Si (001) substrate with a threshold of 1.6 mW at liquid-helium temperature (4.5 K) [39], and an ultra-low threshold of 2.73 μW was obtained under pulsed pumping conditions at room temperature [40]. However, room-temperature CW-pumped microdisk QD lasers with an ultra-low lasing threshold directly grown on planar on-axis Si (001) substrate have not been reported.

In this work, we demonstrate extremely low-threshold lasing in three stacked InAs/GaAs QD microdisk lasers monolithically grown on on-axis Si (001) substrate at room temperature by CW optical pumping. The lasing emission of microdisk lasers with a diameter (D) of ∼2 μm and a sub-wavelength scale $D \sim 1.1$ μm is illustrated, of which an ultra-low threshold ∼3 μW is obtained. Lasing emissions from both the ground state and excited states are observed. The promising lasing characteristics of the microdisk lasers with an ultra-low lasing threshold and small footprint provide a viable route towards large-scale, low-cost integration of laser sources on the Si platform.

2. MATERIAL GROWTH AND FABRICATION

The InAs/GaAs QD microdisk lasers were monolithically grown on planar on-axis Si (001) substrates without any intermediate buffer layer [41]. A 400 nm epitaxial GaAs film was first deposited on the on-axis Si (001) substrate without antiphase boundaries using metal–organic chemical vapor deposition. A detailed description of the epitaxial structure between the active region and the Si (001) substrate, as well as the process of crystal growth, can be found in Refs. [33] and [41]. Figure 1(a) shows a cross-sectional transmission electron microscope (TEM) image of the microdisk structure grown on a planar on-axis Si (001) substrate. The epitaxial structure of the microdisk region is schematically demonstrated in Fig. 1(b). Three stacked well-developed InAs/$In_{0.15}Ga_{0.85}As$/GaAs dot-in-well (DWELL) active layers were separated by a 50 nm GaAs spacer layer and sandwiched by two symmetrical 69 nm $Al_{0.4}Ga_{0.6}As$ cladding layers capped by a 10 nm GaAs layer. Figures 1(c) and 1(d) illustrate the high-resolution TEM images of the three stacked grown InAs/GaAs QD layers and a single QD, respectively. Figure 1(e) shows the atomic distribution profile of In as a function of depth from the surface on the epitaxial chip obtained by x-ray photoelectron spectroscopy (XPS). The QDs monolithically grown on Si present good uniformity with a density of $\sim 4 \times 10^{10}$ cm^{-2}, of which the typical size is 25 nm in D and 8 nm in height. Moreover, the threading dislocation density was estimated at around 10^7 to 10^8 cm^{-2}, determined by atomic force microscopy (AFM) [Fig. 1(f)] and TEM images. Figure 1(g) demonstrates the room-temperature photoluminescence (PL) spectra of the as-grown structure at a range of input power from 3.5 μW to 220 μW, indicating ground state emission (peak at around 1315 nm) was at 1.3 μm telecommunication wavelength band. PL from the excited states and the wetting layer of QDs was observed when increasing the pump power.

Various microdisk patterns were defined by using electron-beam lithography with a ZEP520 electron beam resist. A layer of silicon dioxide (SiO_2) with a thickness of around 120 nm was first deposited on the wafer by plasma-enhanced chemical vapor deposition and used as the hard mask. The microdisk patterns were transferred from the resist into the hard mask using reactive ion etching (RIE). After removing the resist, the hard mask patterns were further transferred through the active region using inductively coupled plasma RIE (ICP-RIE). Then wet etching was used to remove the SiO_2 hard mask and form the supporting pedestal. The fabricated microdisk lasers were characterized in a micro-PL (μ-PL) system at room temperature and were CW optically pumped using a 632.8 nm He–Ne laser with focus spot size of ∼3 μm.

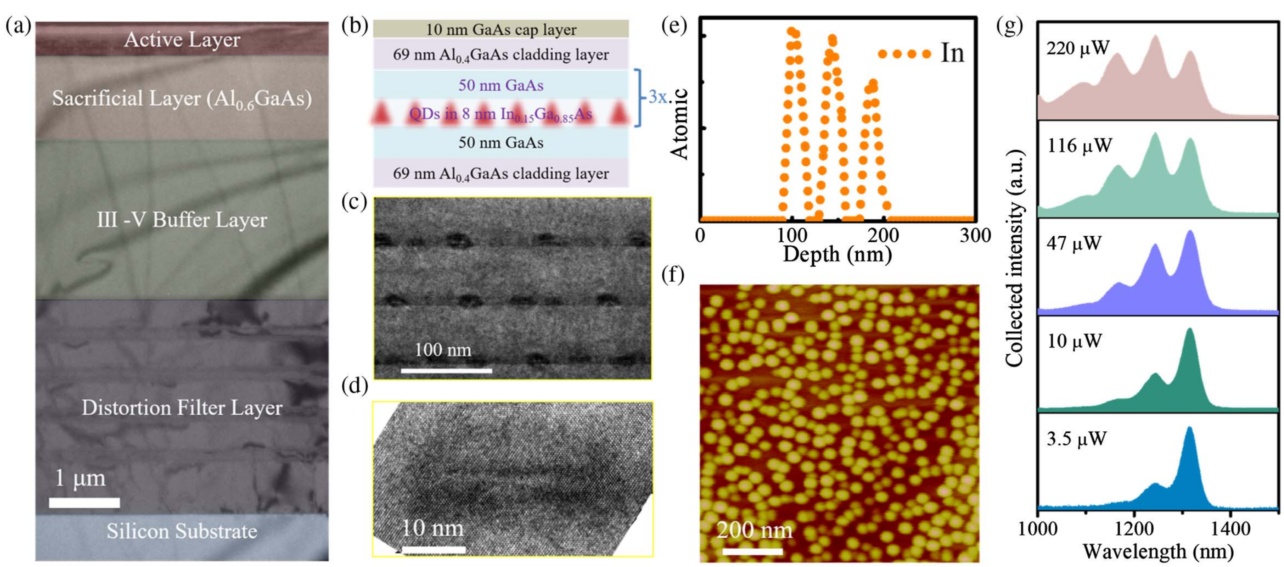

Fig. 1. (a) TEM image of the QD structure grown on on-axis Si (001) substrate. (b) Schematic illustration of the epitaxial structure of the active region. (c), (d) High-resolution TEM images of the three stacked InAs QD layers and a single QD, respectively. (e) Atomic distribution profile of In obtained by XPS. (f) AFM image of uncapped InAs/GaAs QDs grown on Si (001) substrate. (g) Room-temperature PL spectra of the as-grown structure at various input powers.

3. RESULTS AND DISCUSSION

Figure 2(a) shows a schematic diagram of the fabricated microdisk cavity, with three layers of QD embedded inside the active region. A scanning electron microscope (SEM) image of the fabricated microdisk cavity with $D \sim 1.9$ μm is shown in Fig. 2(b), indicating a smooth surface of the active region and ~73.5° sidewall tilt. Figure 2(c) shows the collected PL spectra below and above the lasing threshold of the microdisk with $D \sim 1.9$ μm, indicating a measured free spectral range (FSR) of ~76 nm–89 nm between the adjacent WGMs in the same radial order. The measured FSR is consistent with the calculated value (calculated value: $\mathrm{FSR} = \frac{\lambda^2}{\pi D n_{\mathrm{eff}}} \sim \frac{(1.250\ \mu\mathrm{m})^2}{\pi(1.9\ \mu\mathrm{m})(3.4)} = 77$ nm). Lasing emissions from both the ground state and excited states were obtained, from which the main peak (1263 nm) was located within the first excited state. Excited states lasing emission was also observed for microdisk lasers grown on V-grooved-Si substrate with five stacked InAs QDs [20,21]. The corresponding collected intensity (L-L curve) and full width at half maximum (FWHM) for the emission peak at 1263 nm as a function of input power are demonstrated in Fig. 2(d), which shows the ultra-low threshold of 2.6 ± 0.4 μW obtained. (Note that due to the multimode lasing behavior, the lasing threshold of the emission peak at 1263 nm should be lower than 2.6 ± 0.4 μW; this threshold error came from both the measured power and the curve fitting of measured PL data.) The lasing threshold was determined by the L-L curve. The trend of the FWHM narrowing was obvious, and this was used to judge the lasing behavior. The measured lasing threshold was even lower than those of the InAs QD microdisk lasers directly grown on GaAs or InP substrates [19,42,43]. During the μ-PL measurements, both the broad background and resonant emissions were observed. Background emission can be suppressed by enhancing the coupling between the emitter and microcavity and improving the spatial overlap between the gain material and WGMs. Figure 2(e) demonstrates the curve fitting of the measured spectra above the threshold (4.4 μW), which comprises a spontaneous emission background and cavity emission. Figure 2(f) displays the redshift of the measured lasing peaks with increasing incident pump power induced by thermal effects. A redshift rate of $d\lambda/dP_{\mathrm{pump}} \sim 5.69$ nm/mW was obtained using a linear fit.

By increasing the pump power, the intensity of excited states emission can be stronger than that of the ground state emission, as shown in Fig. 1(g). The higher pump power reveals mode competition between the ground state and excited states of QDs due to gain saturation. Figure 3(a) shows the collected laser spectra of a microdisk laser with $D \sim 2$ μm under various pump powers. Increasing the pump power results in gradual gain saturation of the ground state transition (1317 nm), and lasing switches to the excited state (1240 nm). The ground state gain saturation can be further prevented by increasing the stacked layers of QDs within the active layer [44]. The thresholds of lasing peaks at 1317 nm and 1240 nm are 2.7 ± 0.4 μW and 6.5 ± 0.4 μW, respectively, indicated by the L-L curve [Fig. 3(b)]. The relatively higher lasing threshold of the excited state is a consequence of the larger density of excited states.

One way to obtain single-mode lasing emission is to decrease the D of the microdisk cavity. The FSR becomes larger with a smaller D of the microdisk cavity, which leads to well-separated resonant peaks for single-mode lasing emission (i.e., the FSR is comparable to or larger than the FWHM of the gain spectra). Here, the lasing characteristics of a microdisk laser with $D \sim$ 1.4 μm and a sub-wavelength microdisk laser with $D \sim 1.1$ μm were measured. Figure 4(a) presents the lasing spectra of the microdisk lasers with $D \sim 1.1$ μm and ~1.4 μm, in which both the first- and second-order WGMs are observed with increasing pump power. A much broader measured FSR of 159 nm for the microdisk laser with $D \sim 1.1$ μm (FSR of 116 nm for the $D \sim 1.4$ μm) of the same radial order is observed compared with the FSR presented in Figs. 2(c) and 3(a). A side-mode suppression ratio of 6.5 dB is obtained. The FSR is also much larger than the

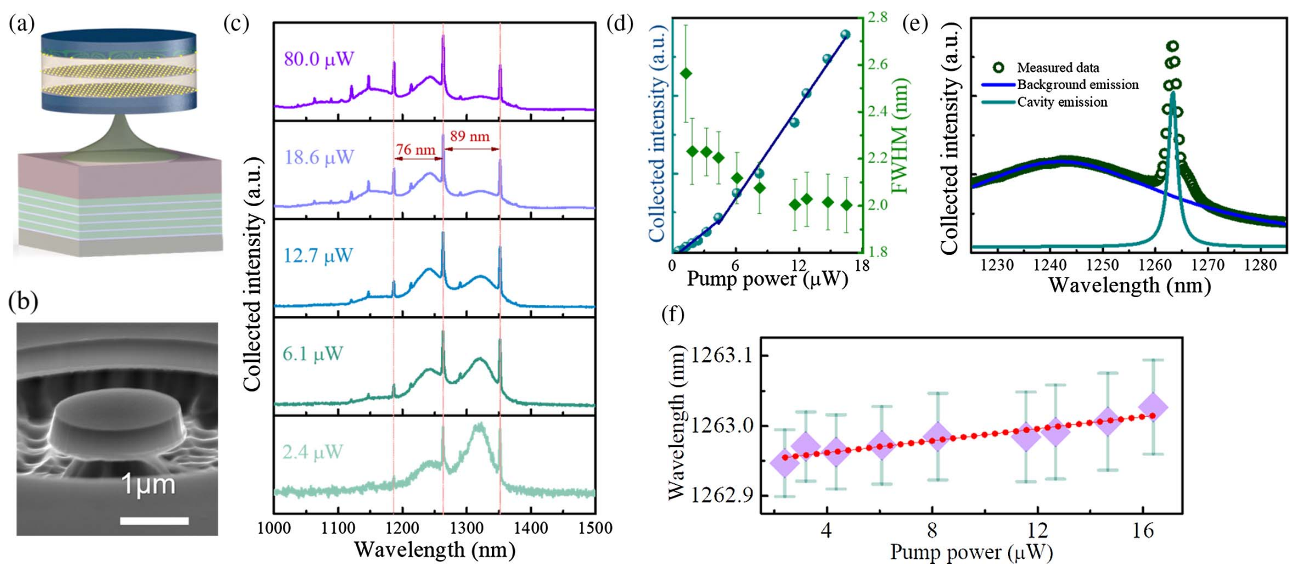

Fig. 2. (a) Schematic diagram of a microdisk laser grown on planar on-axis Si (001) substrate. (b) SEM image of a fabricated microdisk laser. (c) Collected PL spectra below and above the lasing threshold of a microdisk with $D \sim 1.9$ μm. (d) Corresponding collected intensity and mode linewidth as a function of input power for the emission peak at 1263 nm. The lasing threshold is $\sim 2.6 \pm 0.4$ μW. (e) Collected spectra above the threshold (4.4 μW) and curve fitting showing the spontaneous emission background and cavity emission. (f) Measured lasing wavelength under various incident pump powers.

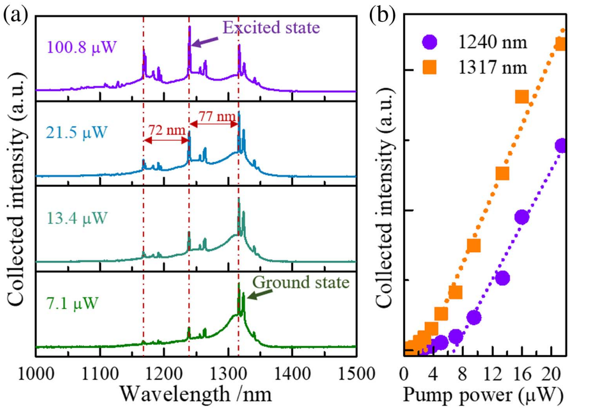

Fig. 3. (a) Measured lasing spectra of the microdisk laser with $D \sim 2\ \mu m$ under various pump powers. Lasing emissions from both ground state and excited states are observed. (b) L-L curve of the emission peaks at 1240 nm (first excited state) and 1317 nm (ground state), respectively.

linewidth (~46 nm) of the ground state emission, which substantially can support one resonate frequency of first-order WGMs within the ground state. In addition, the mode positions (cavity resonate frequencies) are highly dependent on the structural parameters of the cavity. During the optical pumping process, the lasing emission peak from the excited states at 1189 nm (ground state at 1315 nm) dominates the lasing spectra of the microdisk laser with $D \sim 1.1\ \mu m$ ($D \sim 1.4\ \mu m$), as shown in the Fig. 4(a). A lasing peak with weaker intensity of the ground state is also observed for the microdisk laser with $D \sim 1.1\ \mu m$, for which there is not clear mode switching from the ground state to the excited states with the gradual increase in pump power. The lasing in the excited states is due mainly to the mode selection of the sub-wavelength scale microdisk cavity. The inset in Fig. 4(a)

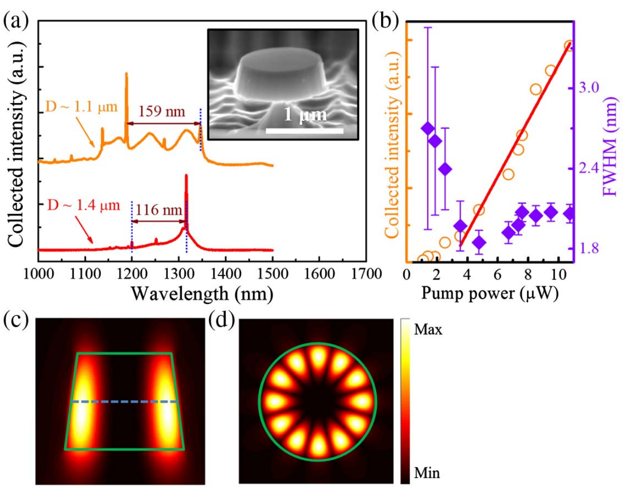

Fig. 4. (a) Measured lasing spectra of the microdisk laser with $D \sim 1.1\ \mu m$ and $\sim 1.4\ \mu m$. The inset SEM image shows the fabricated sub-wavelength scale microdisk laser. (b) L-L curve and FWHM of lasing peak ~1189 nm of the sub-wavelength scale microdisk laser with $D \sim 1.1\ \mu m$, showing the lasing threshold of $\sim 2.9 \pm 0.4\ \mu W$. (c), (d) Calculated cross section and top view of the magnetic field profiles for the $TE_{1,6}$ mode, respectively. The green line represents the boundary of the microdisk, and the blue dashed line demonstrates the central plane of the microdisk.

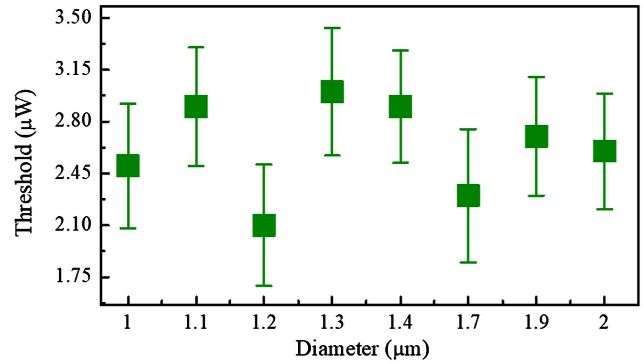

Fig. 5. (a) Thresholds of microdisk lasers with various D. The lasing threshold was derived from the L-L curve of the main lasing peak, and all measured data came from a single microdisk laser.

shows the SEM image of a fabricated sub-wavelength scale microdisk laser. The L-L curve and FWHM of the lasing peak at 1189 nm for the microdisk laser with $D \sim 1.1\ \mu m$ are shown in Fig. 4(b), indicating the lasing threshold of $\sim 2.9 \pm 0.4\ \mu W$. The mode profile of lasing peak at 1189 nm was calculated using the 3D finite-difference time-domain (3D-FDTD) method, and was identified as $TE_{1,6}$. Figures 4(c) and 4(d) show, respectively, the cross section and top view of the calculated magnetic field profiles for $TE_{1,6}$. The green line indicates the boundary of the microdisk resonator, and the blue dashed line demonstrates the central plane of the microdisk. As indicated in Fig. 4(c), the central plane of WGMs is not completely overlapped with the emitter, which may cause the broad background emission of the lasing spectra.

In addition, the thresholds of microdisk lasers with various D from 1 μm to 2 μm are presented in Fig. 5, which indicates low thresholds below 3.5 μW. The lasing threshold of microdisk lasers with smaller D was assumed to be lower due to the decreased gain region. However, the measured lasing thresholds fluctuated with the D, which was highly dependent on the fabrication process factors, such as the width of the supporting pedestal of the microdisk and surface roughness. In addition, the thresholds could have been influenced by the non-uniform distribution of as-grown QDs as well as the difference in gain coefficients of the ground state and excited states.

4. CONCLUSION

In conclusion, we developed InAs/GaAs QD microdisk lasers monolithically grown on on-axis Si (001) substrate. The microdisk lasers were CW optically pumped at room temperature, and an ultra-low lasing threshold of ~3 μW with $D \sim 1.1\ \mu m$ was obtained. Lasing emissions from both the ground state and excited states were demonstrated. The promising lasing characteristics of the microdisk lasers monolithically grown on Si (001) substrate with an ultra-low threshold and small footprint provide a viable route towards the large-scale, low-cost integration of laser sources on a silicon platform.

Funding. The Shenzhen Key Laboratory Project (ZDSYS201603311644527); Shenzhen Fundamental Research Fund (JCYJ20150611092848134, JCYJ20150929170644623); Shenzhen Science and Technology Innovation Fund (KQCX20140522143114399); President's Fund (PF01000154);

National Natural Science Foundation of China (NSFC) (11474365); Foundation of NANO X (18JG01); UK EPSRC (EP/P000886/1, EP/P006973/1); EPSRC National Epitaxy Facility. European project H2020-ICT-PICTURE (780930); Royal Academy of Engineering (RF201617/16/28); Investissments d'avenir (ANR-10-IRT-05, ANR-15-IDEX-02).

Acknowledgment. S. C. thanks the Royal Academy of Engineering for funding his Research Fellowship.

†These authors contributed equally to this work.

REFERENCES

1. D. Liang and J. E. Bowers, "Recent progress in lasers on silicon," Nat. Photonics **4**, 511–517 (2010).
2. M. Asghari and A. V. Krishnamoorthy, "Silicon photonics: energy-efficient communication," Nat. Photonics **5**, 268–270 (2011).
3. A. Rickman, "The commercialization of silicon photonics," Nat. Photonics **8**, 579–582 (2014).
4. D. Thomson, A. Zilkie, J. E. Bowers, T. Komljenovic, G. T. Reed, L. Vivien, D. Marrismorini, E. Cassan, L. Virot, and J. M. Fédéli, "Roadmap on silicon photonics," J. Opt. **18**, 073003 (2016).
5. Z. Wang, K. Van Gasse, V. Moskalenko, S. Latkowski, E. Bente, B. Kuyken, and G. Roelkens, "A III-V-on-Si ultra-dense comb laser," Light: Sci. Appl. **6**, e16260 (2017).
6. A. W. Fang, H. Park, O. Cohen, R. Jones, M. J. Paniccia, and J. E. Bowers, "Electrically pumped hybrid AlGaInAs-silicon evanescent laser," Opt. Express **14**, 9203–9210 (2006).
7. R. Chen, K. W. Ng, W. S. Ko, D. Parekh, F. Lu, T.-T. D. Tran, K. Li, and C. Chang-Hasnain, "Nanophotonic integrated circuits from nanoresonators grown on silicon," Nat. Commun. **5**, 4325 (2014).
8. H. Kroemer, K. J. Polasko, and S. C. Wright, "On the (110) orientation as the preferred orientation for the molecular beam epitaxial growth of GaAs on Ge, GaP on Si, and similar zincblende-on-diamond systems," Appl. Phys. Lett. **36**, 763–765 (1980).
9. H. Kroemer, "Polar-on-nonpolar epitaxy," J. Cryst. Growth **81**, 193–204 (1987).
10. M. Tang, S. Chen, J. Wu, Q. Jiang, K. Kennedy, P. Jurczak, M. Liao, R. Beanland, A. Seeds, and H. Liu, "Optimizations of defect filter layers for 1.3-μm InAs/GaAs quantum-dot lasers monolithically grown on Si substrates," IEEE J. Sel. Top. Quantum Electron. **22**, 1900207 (2016).
11. D. Jung, P. G. Callahan, B. Shin, K. Mukherjee, A. C. Gossard, and J. E. Bowers, "Low threading dislocation density GaAs growth on on-axis GaP/Si (001)," J. Appl. Phys. **122**, 225703 (2017).
12. Z. Mi, P. Bhattacharya, J. Yang, and K. Pipe, "Room temperature self-organised $In_{0.5}Ga_{0.5}As$ quantum dot laser on silicon," Electron. Lett. **41**, 742–744 (2005).
13. J.-R. Reboul, L. Cerutti, J.-B. Rodriguez, P. Grech, and E. Tournié, "Continuous-wave operation above room temperature of GaSb-based laser diodes grown on Si," Appl. Phys. Lett. **99**, 121113 (2011).
14. M. Tang, S. Chen, J. Wu, Q. Jiang, V. G. Dorogan, M. Benamara, Y. I. Mazur, G. J. Salamo, A. Seeds, and H. Liu, "1.3-μm InAs/GaAs quantum-dot lasers monolithically grown on Si substrates using InAlAs/GaAs dislocation filter layers," Opt. Express **22**, 11528–11535 (2014).
15. S. Chen, W. Li, J. Wu, Q. Jiang, M. Tang, S. Shutts, S. N. Elliott, A. Sobiesierski, A. J. Seeds, I. Ross, P. M. Smowton, and H. Liu, "Electrically pumped continuous-wave III-V quantum dot lasers on silicon," Nat. Photonics **10**, 307–311 (2016).
16. Y. Wang, S. Chen, Y. Yu, L. Zhou, L. Liu, C. Yang, M. Liao, M. Tang, Z. Liu, J. Wu, W. Li, I. Rose, A. J. Seeds, H. Liu, and S. Yu, "Monolithic quantum-dot distributed feedback laser array on silicon," Optica **5**, 528–533 (2018).
17. Z. Wang, B. Tian, M. Pantouvaki, W. Guo, P. Absil, J. Van Campenhout, C. Merckling, and D. Van Thourhout, "Room-temperature InP distributed feedback laser array directly grown on silicon," Nat. Photonics **9**, 837–842 (2015).
18. Y. Wan, Q. Li, Y. Geng, B. Shi, and K. M. Lau, "InAs/GaAs quantum dots on GaAs-on-V-grooved-Si substrate with high optical quality in the 1.3 μm band," Appl. Phys. Lett. **107**, 081106 (2015).
19. B. Tian, Z. Wang, M. Pantouvaki, P. Absil, J. Van Campenhout, C. Merckling, and D. Van Thourhout, "Room temperature O-band DFB laser array directly grown on (001) silicon," Nano Lett. **17**, 559–564 (2016).
20. Y. Wan, Q. Li, A. Y. Liu, W. W. Chow, A. C. Gossard, J. E. Bowers, E. L. Hu, and K. M. Lau, "Sub-wavelength InAs quantum dot micro-disk lasers epitaxially grown on exact Si (001) substrates," Appl. Phys. Lett. **108**, 221101 (2016).
21. Q. Li, Y. Wan, A. Y. Liu, A. C. Gossard, J. E. Bowers, E. L. Hu, and K. M. Lau, "1.3-μm InAs quantum-dot micro-disk lasers on V-groove patterned and unpatterned (001) silicon," Opt. Express **24**, 21038–21045 (2016).
22. Y. Wan, Q. Li, A. Y. Liu, A. C. Gossard, J. E. Bowers, E. L. Hu, and K. M. Lau, "Temperature characteristics of epitaxially grown InAs quantum dot micro-disk lasers on silicon for on-chip light sources," Appl. Phys. Lett. **109**, 011104 (2016).
23. J. Norman, M. J. Kennedy, J. Selvidge, Q. Li, Y. Wan, A. Y. Liu, P. G. Callahan, M. P. Echlin, T. M. Pollock, K. M. Lau, A. C. Gossard, and J. E. Bowers, "Electrically pumped continuous wave quantum dot lasers epitaxially grown on patterned, on-axis (001) Si," Opt. Express **25**, 3927–3934 (2017).
24. Y. Shi, Z. Wang, J. Van Campenhout, M. Pantouvaki, W. Guo, B. Kunert, and D. Van Thourhout, "Optical pumped InGaAs/GaAs nano-ridge laser epitaxially grown on a standard 300-mm Si wafer," Optica **4**, 1468–1473 (2017).
25. Y. Han, W. K. Ng, C. Ma, Q. Li, S. Zhu, C. C. Chan, K. W. Ng, S. Lennon, R. A. Taylor, K. S. Wong, and K. M. Lau, "Room temperature InP/InGaAs nano-ridge lasers grown on Si and emitting at telecom bands," Optica **5**, 918–923 (2018).
26. H. Liu, T. Wang, Q. Jiang, R. Hogg, F. Tutu, F. Pozzi, and A. Seeds, "Long-wavelength InAs/GaAs quantum-dot laser diode monolithically grown on Ge substrate," Nat. Photonics **5**, 416–419 (2011).
27. A. Lee, Q. Jiang, M. Tang, A. Seeds, and H. Liu, "Continuous-wave InAs/GaAs quantum-dot laser diodes monolithically grown on Si substrate with low threshold current densities," Opt. Express **20**, 22181–22187 (2012).
28. A. D. Lee, Q. Jiang, M. Tang, Y. Zhang, A. J. Seeds, and H. Liu, "InAs/GaAs quantum-dot lasers monolithically grown on Si, Ge, and Ge-on-Si substrates," IEEE J. Sel. Top. Quantum Electron. **19**, 1901107 (2013).
29. N. Kryzhanovskaya, E. Moiseev, Y. S. Polubavkina, M. Maximov, M. Kulagina, S. Troshkov, Y. M. Zadiranov, A. Lipovskii, N. Baidus, A. Dubinov, Z. Krasilnik, A. Novikov, D. Pavlov, A. Rykov, A. Sushkov, D. Yurasov, and A. Zhukov, "Electrically pumped InGaAs/GaAs quantum well microdisk lasers directly grown on Si (100) with Ge/GaAs buffer," Opt. Express **25**, 16754–16760 (2017).
30. V. Y. Aleshkin, N. Baidus, A. Dubinov, A. Fefelov, Z. Krasilnik, K. Kudryavtsev, S. Nekorkin, A. Novikov, D. Pavlov, I. Samartsev, E. Skorokhodov, M. Shaleev, A. Sushkov, A. Yablonskiy, P. Yunin, and D. Yurasov, "Monolithically integrated InGaAs/GaAs/AlGaAs quantum well laser grown by MOCVD on exact Ge/Si (001) substrate," Appl. Phys. Lett. **109**, 061111 (2016).
31. D. Jung, J. Norman, M. J. Kennedy, C. Shang, B. Shin, Y. Wan, A. C. Gossard, and J. E. Bowers, "High efficiency low threshold current 1.3 μm InAs quantum dot lasers on on-axis (001) GaP/Si," Appl. Phys. Lett. **111**, 122107 (2017).
32. A. Y. Liu, J. Peters, X. Huang, D. Jung, J. Norman, M. L. Lee, A. C. Gossard, and J. E. Bowers, "Electrically pumped continuous-wave 1.3 μm quantum-dot lasers epitaxially grown on on-axis (001) GaP/Si," Opt. Lett. **42**, 338–341 (2017).
33. S. Chen, M. Liao, M. Tang, J. Wu, M. Martin, T. Baron, A. Seeds, and H. Liu, "Electrically pumped continuous wave 1.3 μm InAs/GaAs quantum dot lasers monolithically grown on on-axis Si (001) substrates," Opt. Express **25**, 4632–4639 (2017).
34. N. Lindenmann, G. Balthasar, D. Hillerkuss, R. Schmogrow, M. Jordan, J. Leuthold, W. Freude, and C. Koos, "Photonic wire bonding: a novel concept for chip-scale interconnects," Opt. Express **20**, 17667–17677 (2012).
35. G. Roelkens, D. Van Thourhout, and R. Baets, "High efficiency grating coupler between silicon-on-insulator waveguides and perfectly vertical optical fibers," Opt. Lett. **32**, 1495–1497 (2007).
36. J. E. Bowers, J. T. Bovington, A. Y. Liu, and A. C. Gossard, "A path to 300 mm hybrid silicon photonic integrated circuits," in *Optical Fiber*

Communications Conference and Exhibition (OFC) (IEEE, 2014), pp. 1–3.

37. Z. Wang, C. Junesand, W. Metaferia, C. Hu, L. Wosinski, and S. Lourdudoss, "III-Vs on Si for photonic applications—a monolithic approach," Mater. Sci. Eng. B **177**, 1551–1557 (2012).
38. Y. Wan, Q. Li, A. Y. Liu, A. C. Gossard, J. E. Bowers, E. L. Hu, and K. M. Lau, "Optically pumped 1.3 μm room temperature InAs quantum-dot micro-disk lasers directly grown on (001) silicon," Opt. Lett. **41**, 1664–1667 (2016).
39. B. Shi, S. Zhu, Q. Li, Y. Wan, E. L. Hu, and K. M. Lau, "Continuous-wave optically pumped 1.55 μm InAs/InAlGaAs quantum dot microdisk lasers epitaxially grown on silicon," ACS Photon. **4**, 204–210 (2017).
40. B. Shi, S. Zhu, Q. Li, C. W. Tang, Y. Wan, E. L. Hu, and K. M. Lau, "1.55 μm room-temperature lasing from subwavelength quantum-dot microdisks directly grown on (001) Si," Appl. Phys. Lett. **110**, 121109 (2017).
41. R. Alcotte, M. Martin, J. Moeyaert, R. Cipro, S. David, F. Bassani, F. Ducroquet, Y. Bogumilowicz, E. Sanchez, and Z. Ye, "Epitaxial growth of antiphase boundary free GaAs layer on 300 mm Si (001) substrate by metalorganic chemical vapour deposition with high mobility," APL Mater. **4**, 083514 (2016).
42. H. Cao, J. Y. Xu, W. H. Xiang, Y. Ma, S. H. Chang, S. T. Ho, and G. S. Solomon, "Optically pumped InAs quantum dot microdisk lasers," Appl. Phys. Lett. **76**, 3519–3521 (2000).
43. S. Zhu, B. Shi, Y. Wan, E. L. Hu, and K. M. Lau, "1.55 μm band low-threshold, continuous-wave lasing from InAs/InAlGaAs quantum dot microdisks," Opt. Lett. **42**, 679–682 (2017).
44. A. Zhukov, A. Kovsh, N. Maleev, S. Mikhrin, V. Ustinov, A. Tsatsul'nikov, M. Maximov, B. Volovik, D. Bedarev, Y. M. Shernyakov, P. S. Kop'ev, Z. I. Alferov, N. N. Ledenntsov, and D. Bimberg, "Long-wavelength lasing from multiply stacked InAs/InGaAs quantum dots on GaAs substrates," Appl. Phys. Lett. **75**, 1926–1928 (1999).